Arabian Journal of Chemistry 16 (2023) 105253

Contents lists available at ScienceDirect

Arabian Journal of Chemistry

journal homepage: www.sciencedirect.com

Original article

New activated carbon derived from *Gundelia tournefortii* seeds for effective removal of acetaminophen from aqueous solutions: Adsorption performance

Shekoofe Mokhtaryan [a], Abbas Khodabakhshi [a], Ramezan Sadeghi [a], Heshmatollah Nourmoradi [b], Kobra Shakeri [a], Sara Hemati [a,c], Fazel Mohammadi-Moghadam [a,d,*]

[a] Department of Environmental Health Engineering, School of Health, Shahrekord University of Medical Sciences, Shahrekord, Iran
[b] Department of Environmental Health Engineering, School of Health, Ilam University of Medical Sciences, Pajouhesh Ave., Ilam 6939177143, Iran
[c] Student Research Committee, Shahrekord University of Medical Sciences, Shahrekord, Iran
[d] Social Determinants of Health Research Center, Shahrekord University of Medical Sciences, Shahrekord, Iran

ARTICLE INFO

Article history:
Received 12 March 2023
Accepted 6 September 2023
Available online 10 September 2023

Keywords:
Adsorption
Activated carbon
Acetaminophen
Gundelia tournefortii seeds
Aqueous solutions

ABSTRACT

Pharmaceuticals as one of the emerging pollutants in water systems are a global environmental concern. This study aims to synthesize a new activated carbon from Gundelia tournefortii seeds (ACGT) for effective removal of acetaminophen (ACT) from aqueous solutions. The synthesized adsorbent was characterized by different techniques, namely FESEM, EDX, XRD, FTIR, BET, TGA, and pHpzc. The effects of experimental parameters such as pH, adsorbent dosage, initial concentration, contact time and ionic strength on the ACT adsorption were investigated. Optimization studies revealed that the maximum removal (98.31%) of ACT was obtained at 30 min of contact time, 0.25 g/L adsorbent, 20 mg/L Ca^{2+}, pH 4.0 and temperature 25C. For predicting ACT adsorption on synthetized adsorbent, isotherm, kinetic, and thermodynamic characteristics were determined. The equilibrium data were well represented by Freundlich model (R^2 = 0.97) and kinetics data were well fitted by the pseudo-second order model. The thermodynamic analysis discovered that the adsorption process was endothermic and spontaneous. Overall, the development of the ACGT can be a promising adsorbent for ACT removing from aqueous solutions.

1. Introduction

Pharmaceuticals in water systems are a global environmental concern (Marcelino et al., 2020, Yang et al., 2021). Such compounds as an important group of chemicals are used in human and veterinary medicines and enter into the aquatic environments through improper disposal (Kekes et al., 2020, Kumari and Kumar 2021). Acetaminophen (ACT) as an over-the-counter (OTC) medication is easily available to the public in many countries and commonly taken to relieve pain and treat fever (Nourmoradi et al., 2018, Eslami et al., 2020, Kekes et al., 2020). Global production of ACT is reported to be>145,000 tons per year (Nourmoradi et al., 2018, Kumari and Kumar 2021).ACT is an active ingredient in the WHO list of the most important drugs (Żółtowska-Aksamitowska et al., 2018). This drug is considered toxic to aquatic organisms and human due to its phenolic groups (Kumari and Kumar 2021). Overusing of ACT can cause acute liver failure (Dadkhah et al., 2016, Nourmoradi et al., 2018) and repeated long-term use can lead to chronic diseases, cancer, and antibiotic resistance (Marcelino et al., 2020). Also, the presence of the drug in aquatic environments causes biological accumulation and continuous presence in the food chain (Natarajan et al., 2022), creating oxidative stress, reproductive and growth disorders, changes in sex hormones along with increasing mortality rate in aquatic species (Akay and Tezel 2020). The maximum allowable dose of ACT in adults is 4 g/day (Eichenbaum et al., 2020, Rahman and Nasir 2020). Some of it is excreted as glucuronide, sulfate, cysteine and the rest is remaining unchanged and enters into the aquatic envi-

* Corresponding author at: Department of Environmental Health Engineering, School of Health, Shahrekord University of Medical Sciences, Shahrekord, Iran.
E-mail address: fm.moghadam@skums.ac.ir (F. Mohammadi-Moghadam).

Peer review under responsibility of King Saud University. Production and hosting by Elsevier.

Production and hosting by Elsevier

https://doi.org/10.1016/j.arabjc.2023.105253
1878-5352/

ronment through domestic, industrial, and hospital wastewaters (Rahman and Nasir 2020). Many studies show that drug compounds are not completely removed from streams during conventional wastewater treatment (Żółtowska-Aksamitowska et al., 2018). In general, the concentration of ACT in domestic wastewaters is estimated to be around 30–40 μg/L, while the drug has been detected in higher concentrations (about 400 μg/L) in the pharmaceutical industry and hospital effluents (Rahman and Nasir 2020). Therefore, due to high consumption and presence in the ecosystem and the adverse effects of that on human health and the environment, elimination of ACT in the ecosystem, especially in aquatic environments, is essential (Amouzgar et al., 2017). Various methods including ultrasonic irradiation (Nourmoradi et al., 2018) ozonation (Iovino et al., 2015) electrochemical degradation (Nourmoradi et al., 2018), photocatalytic degradation (Ahmed et al., 2021), adsorption (Bello et al., 2020, Parus et al., 2020), advanced oxidation processes (Fahmy et al., 2020) and biological treatment (Parus et al., 2020) have been used to remove drugs from effluents and aqueous media,. These methods have several disadvantages including high capital and maintenance costs, a complex operating procedure, and the production of toxic secondary by-products. Among the remediation methods, adsorption technology has gotten a lot of attention because it is easy to use, low cost, effective, and has a wide range of adsorbents that can be used (Yosef et al., 2020, yosef et al., 2021). Moreover, adsorption is seen as one of the most promising techniques that is also good for the environment (Fahmy et al., 2022, Mohamed et al., 2022). Using agricultural waste as low cost and abundant precursors to remove pollutants is a very smart strategy (Mestre et al., 2009, Dadkhah et al., 2016). Many studies have been conducted in this field for the production of activated carbon to remove pharmaceutical substances (Baccar et al., 2012, Cunha et al., 2020, Ouyang et al., 2020). *Gundelia tournefortii* (GT) is a flowering, shrubby, thorn-like plant belonging to the genus Gundelia and the family Asteraceae. This plant is native to Iran, Turkey, Azerbaijan, Egypt, Cyprus, Jordan, and other western regions. GT found as a wild herb growing during late winter and early spring on the hills in the central and western parts of Iran. The stem of this plant is used in Iran as a food and also as a medication in traditional medicine (Hajizadeh-Sharafabad et al., 2016).In this study, for the first time, GT seed pomace has been used to produce activated carbon for ACT removal from aqueous solution. However, to the best of our knowledge, no studies have been reported on activated carbon from Gundelia tournefortii (ACGT) for the removal of ACT from aqueous system. Therefore, the objectives of the present study were to prepare and characterize ACGT and assess the feasibility of utilizing them as a new low-cost adsorbent for the removal of ACT from aqueous solutions. The adsorption behavior of ACT to ACGT, including the adsorption kinetics, isotherms, thermodynamics, and the factors potentially influencing the adsorption, were investigated. Finally, desorption and regeneration trials were performed to determine the adsorbent's recovery, as well as their reusability.

2. Materials and methods

2.1. Chemicals and materials

Gundelia tournefortii (GT) seeds were collected from local area (Shahrekord, Iran). The acetaminophen (ACT, ≥99.0% purity) was purchased from Sigma Aldrich, USA. The physicochemical properties of the ACT are presented in the supplementary materials (See Appendix A: Table S1). Other chemicals such as ferric chloride ($FeCl_3$) > 96%, ferrous sulfate ($FeSO_4$) 99.5%, sodium hydroxide (NaOH) 98%, ethanol (C_2H_5OH) 99%, phosphoric acid (H_3PO_4) 80% and calcium chloride ($CaCl_2$) were purchased from Merck, Germany. Double-distilled water was used for preparation of solutions and experiments.

2.2. Preparation of activated carbon

First, GT seeds were washed with distilled water. After drying, their oil was extracted with an oil-pressing machine, and the remaining were used to prepare activated carbon. In order to remove impurities and reduce alkalinity, GT seed waste were soaked for 24 h in H_3PO_4 at room temperature (1:1 wt ratio with 50 wt%) (González-Hourcade et al., 2022). Then washed several times with distilled water and dried in an oven at 105 °C for 24 h (Nourmoradi et al., 2018). After that, the samples were carbonized in a muffle furnace for 1 h at 700 °C. After heating, the obtained carbonized material were gradually cooled and washed with distilled water until the pH became neutral. The obtained activated carbon was dried overnight at 105 °C (Klasson et al., 2010). Finally, the activated carbon was sieved with a standard mesh of 37–70 (200–500 μm) (Nourmoradi et al., 2018). The carbon (activated carbon derived from GT seeds) was designated as ACGT.

2.3. Adsorption experiments

All experiments for ACT adsorption onto ACGT were done in 50 ml Erlenmeyer flasks. The experimental variables in this study were ACT concentration in (10–100 mg/L), contact time (10–60 min), pH (2–9), adsorbent dose (0.5–2 g/L), and ionic strength (20–80 mg/L Ca^{2+}). Before adsorbent addition, the initial pH of the ACT containing solutions was adjusted by dilute NaOH or H_2SO_4. In all adsorption tests, the samples were shaked at 200 rpm. A calibrated pH meter was used for the measurement of pH. At the end of each adsorption experiment, the adsorbent was separated from suspension using Cellulose Acetate (CA) membrane filter and vacuum filter. The concentrations of ACT were determined using a DR6000 spectrophotometer at 243 nm. Finally, the adsorption capacity of ACT on activated carbon was obtained according to the Eq. (1):

$$q_e = \frac{(C_o - C_e) \times V}{M} \quad (1)$$

In the above equation, q_e is the adsorption capacity of activated carbon (mg/g), C_0 and C_e are the initial and final concentrations of the ACT (mg/L), V is the volume of solution (L) liters and M is the mass of activated carbon (g), respectively (Mohan et al., 2011, Nourmoradi et al., 2018).

2.4. Adsorbent characterization

The morphology of ACGT and raw *Gundelia tournefortii* (RGT) were determined by Field emission Scanning electron microscopy (FESEM) measurements and energy dispersive X-ray spectroscopy (EDX). Fourier transform infrared (FT-IR) spectroscopy (Nicolet Avatar 360, Nicolet, USA) was used to explore the chemical groups on the AC and ACGT in the region 4000–400 cm^{-1}. Particle surface area and porous properties of the AC and ACGT were examined by Brauner-Emmett-Teller (BET) analysis. The texture properties of the ACGT were analyzed with the aid of X-Ray Diffraction (XRD) (model PW 1730) with Cu Kα radiation within 2θ range of 10–80. Thermogravimetric analysis (TGA) of ACGT obtained from PerkinElmer Pyris Diamond 6000 analyzer under a nitrogen atmosphere using a heating range of 20–900 ℃. The pHzpc of ACGT was measured by drift method proposed by Liu et al. (2011) (Liu et al., 2011).

2.5. Adsorption isotherm studies

Adsorption isotherms are useful models for determining adsorbent surface properties, pollutant uptake mechanisms, and understanding the adsorption system. The findings of ACT adsorption onto ACGT were studied by Langmuir, Freundlich and Dubinin–Radushkevich (D-R) isotherms (Inbaraj et al., 2021, Inyinbor et al., 2023). The adsorbent is assumed to be uniformly covered by a monolayer in the Langmuir model. Langmuir isotherm is given through Eq. (2):

$$\frac{C_e}{q_e} = \frac{C_e}{Q_m} + \frac{1}{bQ_m} \tag{2}$$

Where Q_m is the maximum adsorption capacity (mg/g) and b is an isotherm constant (L/mg). The former and latter are attained from the slope and y-intercept of C_e/q_e vs. C_e, respectively (Mohammadi-Moghadam et al., 2013).

For the Freundlich isotherm, multi-layer adsorption can occur on a variety of adsorbent surfaces, Eq. (3):

$$\log q_e = \log K_f + \frac{1}{n}\log C_e \tag{3}$$

Where K_f (L/g) and n represent ACT uptake ability and intensity, respectively. K_f and n are found from the y-intercept and slope of ln q_e vs. C_e, respectively (Natarajan et al., 2022).

The Dubinin- Radushkevich (D-R) isotherm is used to distinguish between physisorption and chemisorption. Eq. (4):

$$lnq_e = lnq_m - \beta\varepsilon^2 \tag{4}$$

Where, q_m (mg/g) is the theoretical ACE uptake onto adsorbent at saturation state, β (kJ/mol) is a fixed value associated to adsorption energy, and ε is the Polanyi potential, obtained by Eq. (5):

$$\varepsilon = RTln(1 + \frac{1}{c_e}) \tag{5}$$

Where, R is the ideal gas law constant (8.314 J/mol.K) and T (K) is the absolute temperature of the aqueous media. The y-intercept and slope of ln q_e versus ϵ^2 i is used to obtain q_m and β, respectively. The parameter of E, the mean uptake energy, is achieved by Eq. (6).

$$E = \frac{1}{\sqrt{2\beta}} \tag{6}$$

E values of < 8 kJ/mol, 8–16 kJ/mol and >16 kJ/mol indicate physisorption, chemical ion exchange and chemisorption, respectively (Inyinbor et al., 2023).

2.6. Adsorption kinetics studies

To determine the adsorption kinetics, the contact time data for ACT removal onto ACGT was investigated by pseudo-first order, pseudo-second order and intraparticle diffusion kinetic models (Ali et al., 2022). Eq. (7) is used to calculate the pseudo-first model.

$$Ln(q_e - q_t) = Lnq_e - K_1 t \tag{7}$$

Where, q_e and q_t refer to adsorbed ACT (mg/g) at equilibrium and time t, respectively, and K_1 (1/min) is the adsorption rate constant, K_1 and q_e q_e were determined from the slope and y-intercept of a semi-log plot of Ln (q_e-q_t) versus t t, respectively.

The pseudo-second order model is characterized by the Eq. (8):

$$\frac{t}{q_t} = \frac{1}{K_2 q_e^2} + \frac{t}{q_e} \tag{8}$$

Where, the pseudo-second order rate constant, K_2 K_2(g/mgmin) and q_e are calculated from the y-intercept and slope of a plot of t/q_t vs. t, respectively.

The intraparticle diffusion kinetic model is presented by Eq. (9):

$$q_t = K_{id} t^{\frac{1}{2}} + C \tag{9}$$

Where, K_{id} (g/mg.min$^{1/2}$) is the intraparticle diffusion kinetic model rate constant and C C(mg/g) is associated with boundary layer thickness. C C and K_{id} K_{id} are obtained via the y-intercept and slope of q_t q_t vs. $t^{1/2}$ $t^{1/2}$, respectively (Mojiri et al., 2019, Kollarahithlu and Balakrishnan 2021).

2.7. Thermodynamic study

The thermodynamic variables associated with ACT adsorption onto ACGT between 283 K and 318 K were determined using Eqs (10)–(13).

$$\Delta G = -RTLnK \tag{10}$$

$$K = \frac{q_e}{C_e} \tag{11}$$

$$\Delta G = \Delta H - T\Delta S \tag{12}$$

$$LnK = \frac{\Delta S}{R} - \frac{\Delta H}{RT} \tag{13}$$

Where K K is the equilibrium constant obtained from the Langmuir isotherm model. ΔG (J/Kmol), ΔH (J/Kmol) and ΔS (J/Kmol) represent the Gibbs free energy, enthalpy and entropy change due to adsorption, respectively. ΔS and ΔH were obtained from the y-intercept and slope of plotting Ln K Ln K vs. 1/T, per 1/T Eq. (13), respectively (Natarajan et al., 2022).

3. Results and discussion

3.1. Characterization of/ structural and morphological study

3.1.1. FESEM analysis

The morphology and surface element distribution of RGT and ACGT were determined by FE-SEM equipped with an Energy-dispersive X-ray spectroscopy detector (EDS). Fig. 1 a depicts the raw carbon surface, which has a uniform distribution with a spherical, smooth surface and regular structure. After activation treatment, several pores shaped on ACGT surface (Fig. 1.b). The pores development was due to the activation process via H_3PO_4 as activating agent. The use of H_3PO_4 may have resulted in the improvement of ACGT surfaces texture and active cavities development during activation (Mojiri et al., 2019). Pores of varying dimensions may provide high surface area for adsorption of ACT. Also, the shape shows the presence of gaps and channels that help to absorb and trap ACT. Some mineral elements (Ca-S-K) were removed from the RGT during the activation process. The presence of P in EDX spectrum confirmed the successful incorporation of P onto ACGT (Fig. 2).

3.1.2. XRD analysis

XRD is a good fingerprint-appropriate characterisation technique that is used to examine phase and crystal structure. (Darweesh et al., 2022, Xue et al., 2022). Fig. 3 show XRD pattern of the activated carbon sample. For this purpose, the diffraction data were generated by exposing the adsorbent sample to Cu-Kα X-ray radiation (λ = 1.54185 Å) operating at 40 kV and 44 mA. The XRD data were obtained at a diffraction region of 2θ from 10° to 80°. The existence of a peak at ~ 25° in the XRD spectra revealed the presence of amorphous or crystalline carbon (Khalil et al., 2013). Because of the amorphous structure of the adsorbent, the ACT molecules could more easily penetrate the surface. The

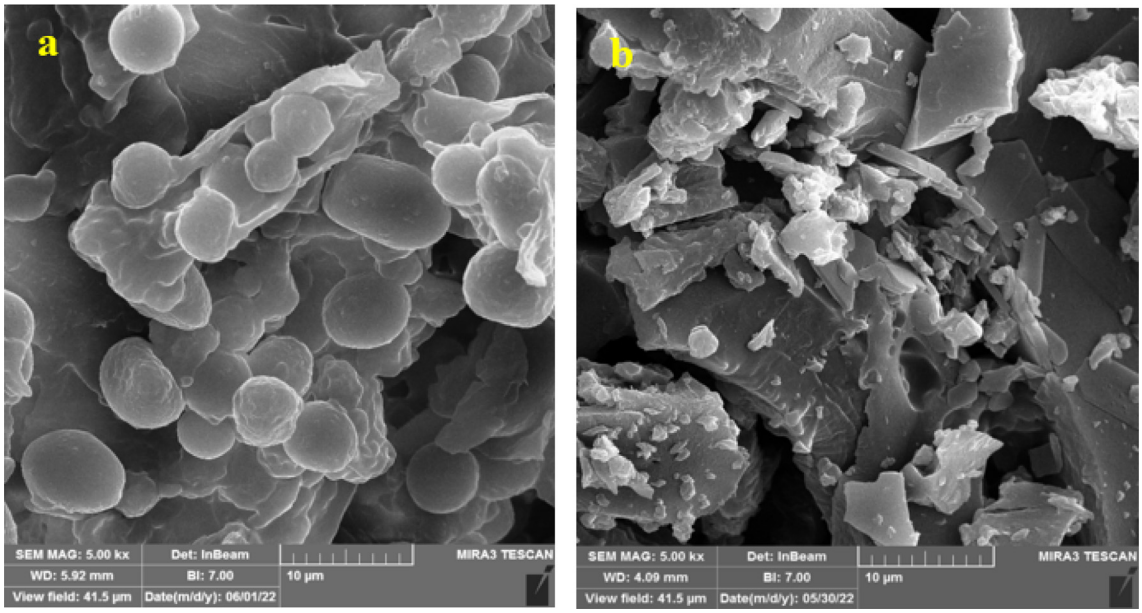

Fig. 1. FESEM of (a) RGT and (b) ACGT.

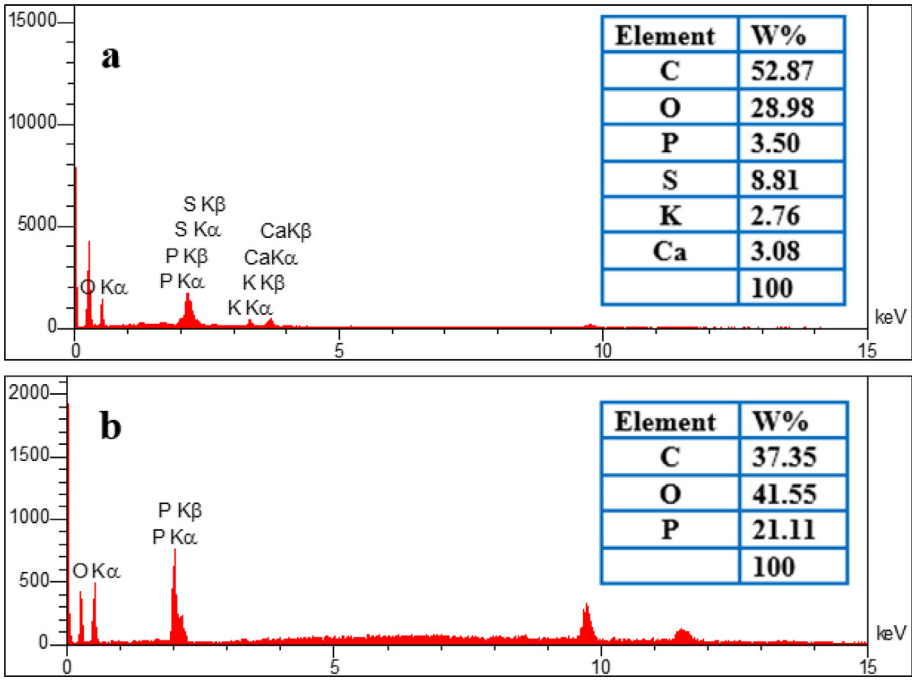

Element	W%
C	52.87
O	28.98
P	3.50
S	8.81
K	2.76
Ca	3.08
	100

Element	W%
C	37.35
O	41.55
P	21.11
	100

Fig. 2. EDX spectra for (a) RGT and (b) ACGT.

slight variations in diffraction peak intensity are due to varying degrees of hydration.

3.1.3. FTIR analysis

The main characteristics functional groups present on the GT surface before and after activation were identified using FT-IR spectroscopy. The FTIR spectra of the RGT and ACGT are given in Fig. 4. FTIR analysis of activated carbon was performed at the 500–4500 cm^{-1} range. The main types of atoms that alter the surface properties of ACs through the creation of functional groups are oxygen, nitrogen, and hydrogen. In ACGT, the broad band observed at 3457 cm^{-1} indicates the presence of –OH group. The absorption peaks observed at 2917 and 2658 cm^{-1} correspond to the stretching vibration of C–H group. The appeared band at 1750 cm^{-1} is assigned to the carbonyl-stretching group (C = O) (Mojiri et al., 2019). The peak at 1612 cm^{-1} can be attributed to the bending vibration of –NH group (Fahmy et al., 2018). The band at 1087 cm^{-1} is related with the C–O stretching vibration of phenolic, carboxylic, and alcoholic groups (Inbaraj et al., 2021). The peak located at 1622 cm^{-1} indicates the C–C band of the aromatic rings which may form through the decomposition of the C = H bond at high carbonization temperatures (Thabede et al., 2020). Free OH groups are located at 3651 cm^{-1} for alcohols, 3617 cm^{-1} for phenols and 3457 cm^{-1} for carboxylic acids. A strong absorption peak

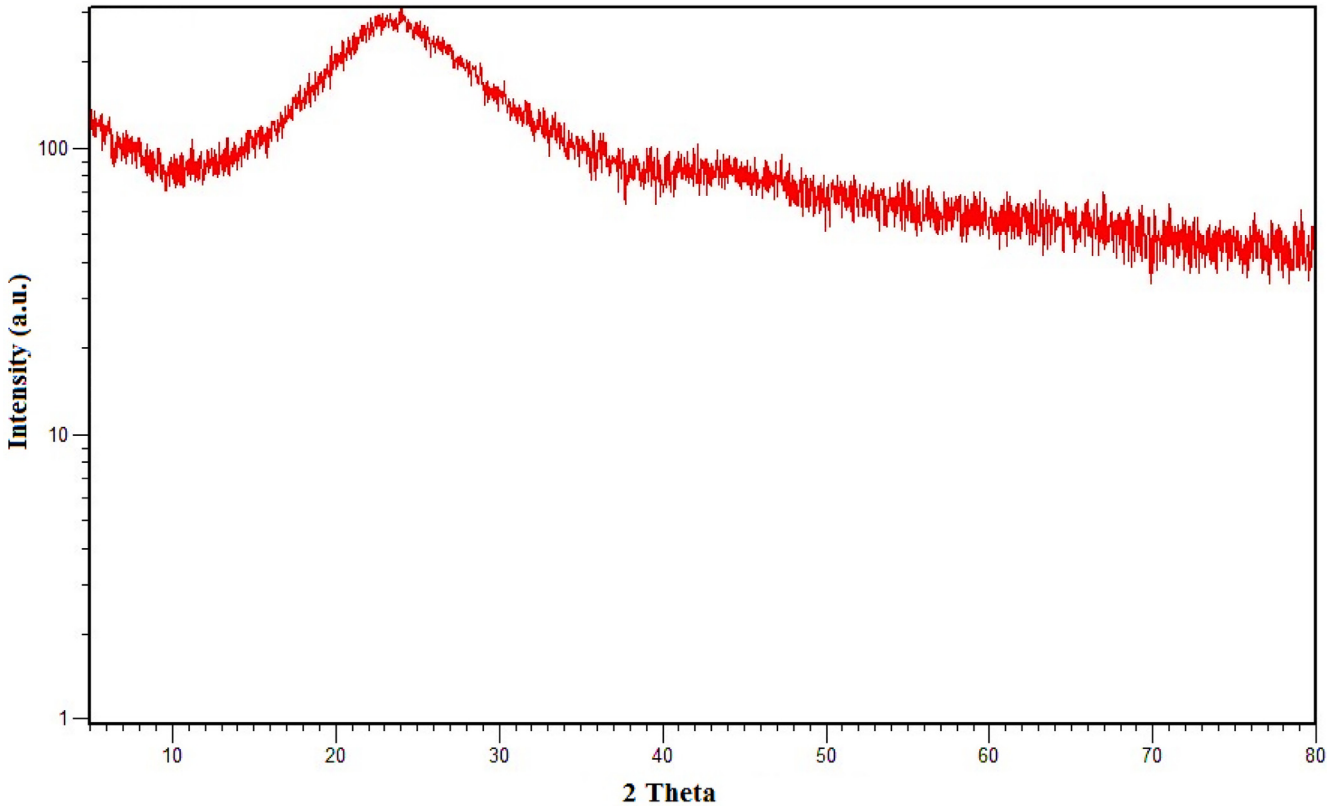

Fig. 3. XRD spectra of ACGT.

at 1591 cm^{-1} corresponds to the N = H bond (Fahmy et al., 2018). Bands around 868 cm^{-1} and 485 cm^{-1} relate to Si-OH and Si-O-Si bands that show clearly the height of these peaks increasing after acidic treatment (Fahmy et al., 2020, Rahman and Nasir 2020). The bands that appear between 739.38 and 1245.21 cm^{-1} in ACGT may be attributed to the presence of phosphorus species in the samples during activation with H_3PO_4 (Kharrazi et al., 2021).

3.1.4. Surface area and porosity analysis by BET-N2 method

BET data shows that the surface area of RGT was 2.88 m^2/g whilst ACGT was 260.44 m^2/g. The effectiveness of physicochemical activation exerted in this study is confirmed by relatively high of BET surface area together with pore volume. Chemically and thermally activation processes developed the porous structure, increased BET surface area and decreased average pore diameter compared with the non– pretreated sample (Kharrazi et al., 2021). The detailed results of the pore structures are found in Table 1.

The N_2 adsorption–desorption isotherms of RGT and ACGT as function of relative pressure are shown in Fig. 5. According to IUPAC classification, the obtained adsorption isotherm profile could be classified as type III for RGT, which describe adsorption on macroporous adsorbents with weak adsorbate-adsorbent interactions (Mohan et al., 2011) (Fig. 3a). Also, adsorption isotherm profile for ACGT was type I, which is typical of a microporous material (Fig. 3b) (Silva et al., 2018).

3.1.5. TGA analysis

TGA was used in this study to determine the thermal stability of ACGT by measuring the weight change that occurred when the samples were heated in an inert N_2 atmosphere. Fig. 6 showed the mass loss (TGA) and derivative mass loss (DTG) curves of ACGT. For ACGT, a three-step degradation pattern was observed with the first-step involving a loss of 7.32% moisture at a temperature < 200 ℃, followed by a 6.69% reduction in weight between 200 and 400 ℃. The second-step it may be attributed to loss of cellulose and hemicellulose residues as well as decomposition of organic ligands. DTA curve showed an endothermic peak at 100℃ which confirmed the elimination of water molecules. Destruction of the organic portion is also confirmed by the presence of a weak exothermic peak in DTA curve. At 400–800 ∘C, a substantially larger weight loss of 32.99% was recorded in the third step, accounting for devolatilization of thermally stable volatile compounds, carbon oxidation, and lignin degradation. This weight loss appeared with a strong exothermic peak (550 ℃) in the DTA curve (Alorabi et al., 2020). At 862 ℃, a final residual mass of 53% was obtained.

3.1.6. pH at point of zero charge (pHpzc)

pHpzc values are given in Fig. 7. The pzc is defined as the pH where the net surface charge resulting from the adsorption of H_3O^+ and OH^-, is zero. The surface of material will be negatively charged at pH > pH_{pzc} and positively charged at pH < pH_{PZC}. The higher the surface acidity, the lower the pHpzc will be. The pHpzc was 5 for ACGT. This value indicates that the adsorbent has acidic character adsorption of anions being enhanced at pH less than pHpzc (Lung et al., 2021). The activated carbon matrix contains oxygen, hydrogen, and nitrogen. The presence of oxygen in surface functions such as carboxyls, carbonyls, and phenol on activated carbon surfaces is well known. Although surface functional groups cover only a small portion of the activated carbon surface, they have a significant impact on the adsorption and reactivities of activated carbons (Mohan et al., 2011, Norouzi et al., 2018).

3.2. Effect of solution pH

Adsorption was carried out in the pH ranging from 3 to 9 to ascertain the effect of pH on the adsorption of ACT (Fig. 8). In general, with increasing pH, the ACT removal efficiency was decreased.

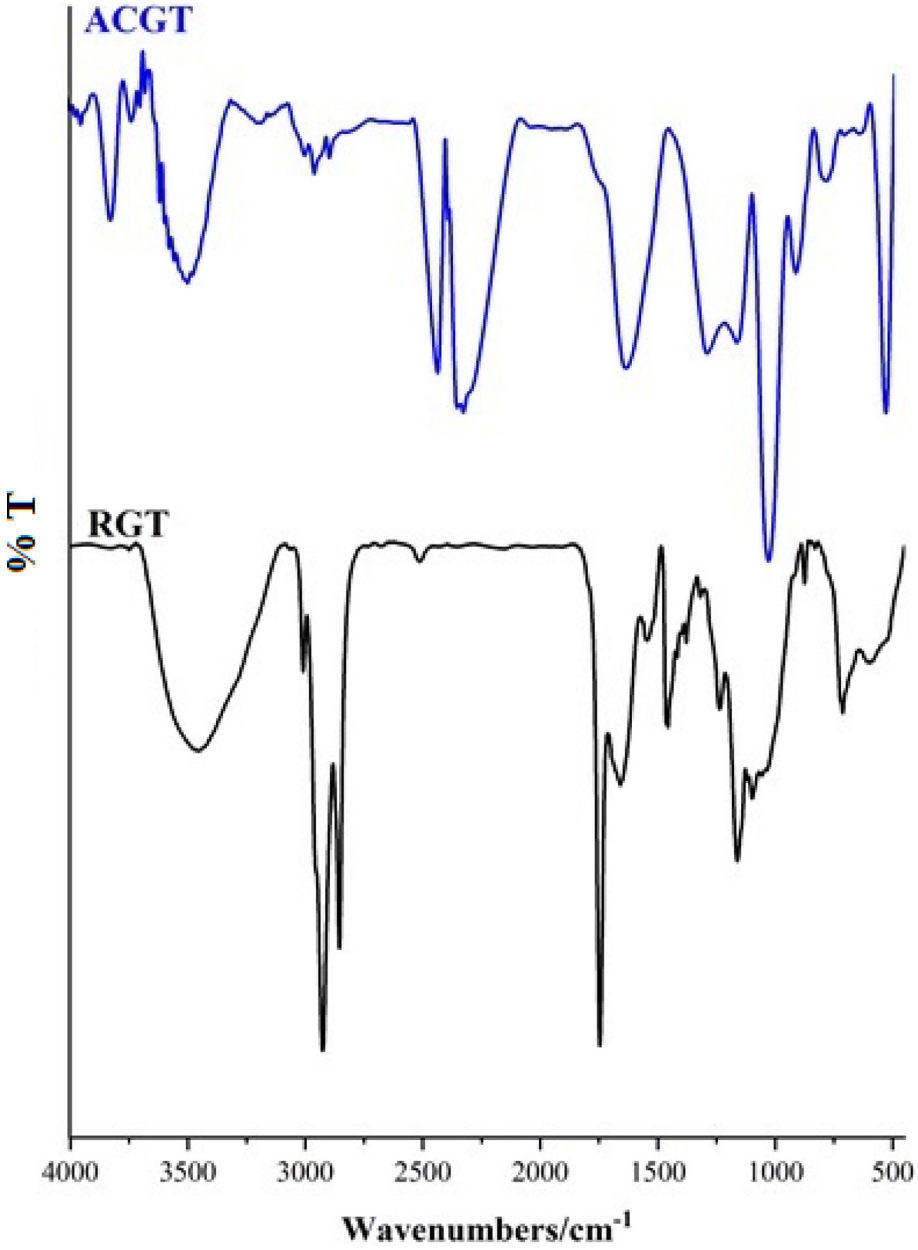

Fig. 4. FT-IR analysis of RGT and ACGT.

Table 1
Surface area and pore characteristics of the samples.

Sample	BET surface area (m^2/g)	Total pore volume (cm^3/g)	Average pore diameter (nm)
RGT	2.88	0.0080659	11.182
ACGT	260.44	0.1273	1.9555

The optimum removal of ACT was observed at pH 4. In the present study, it was found that the pH of the solution is very effective in achieving the maximum removal rate. Variation of pH influencing the nature of ions solution, which can change the structure of the adsorbent surface charges and finally adsorption efficiency. Weak electrolytes, such as ACT with pKa = 9.38, can exist in both ionized and non-ionized forms depending on the pH of the solution. This compound mainly remains in solution at pHs below 9.38 as neutral (non-ionized) species. And when the pH of the solution exceeds 9.38, the dissociation of ACT increases and it becomes ionized. At pH < pKa, ACT exists in the protonated form, which helps in easier adsorption. In the present study, the absorption efficiency decreased with increasing pH, which is due to the competition of hydroxyl ion with ACT for adsorption on the positively charged adsorbent. It is also possible that hydrophobic interactions are the main mechanism of ACT adsorption. Similarly, there is a reduction in adsorption after pH 5.0 because of repulsion between negatively charged adsorbent and anionic acetaminophen molecules. Lung et al. (2021) and Natarajan et al. (2022) also reported similar results so that the removal efficiency of ACT decreased with increasing pH (Lung et al., 2021, Natarajan et al., 2022). Similar results have been reported in the study of Normoradi et al. (2018). They reported that it is due to the competition of hydroxyl ions with ACT for adsorption on the adsorbent (Nourmoradi et al., 2018). A study conducted by Wong et al (2018) showed that no significant difference was observed between pH 3–7 and the optimal

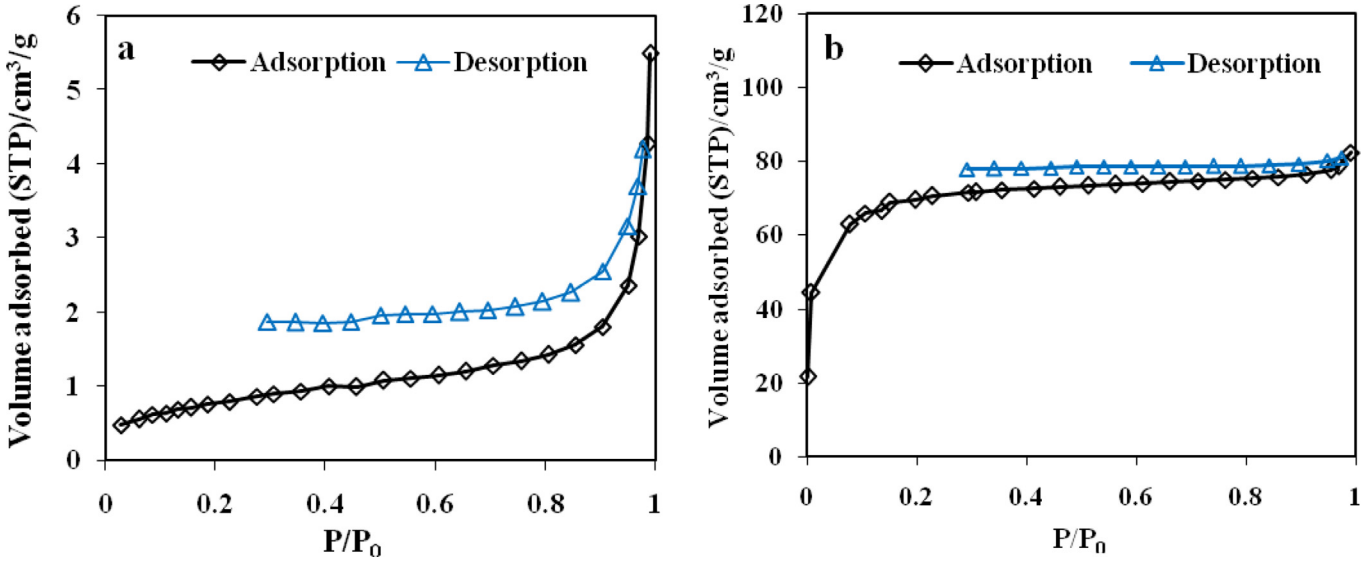

Fig. 5. N_2 adsorption/desorption isotherms at 77 K, (a) RGT, (b) ACGT.

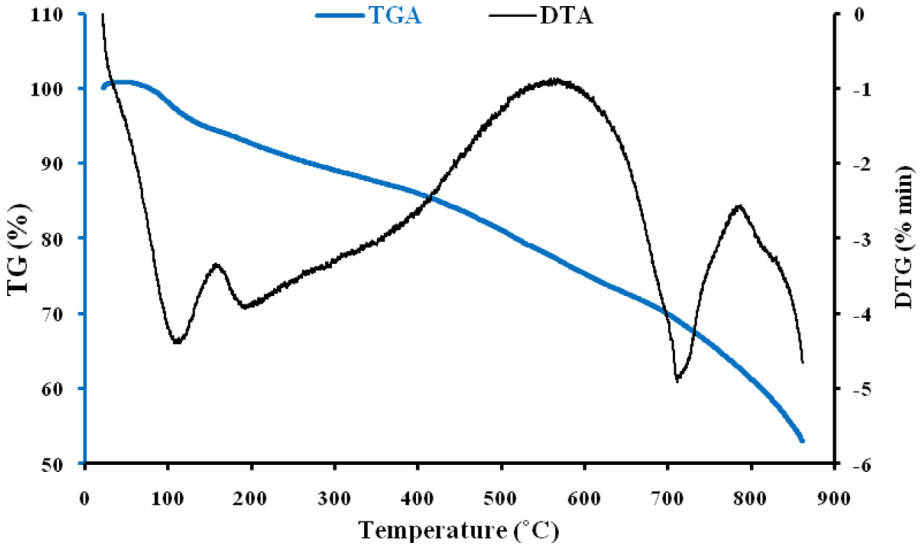

Fig. 6. Thermogravimetric analysis (TGA) curve of ACGT.

efficiency of ACT removal was obtained at pH = 3. It was also observed that the removal efficiency decreased from pH 9 to 11 due to the electrostatic interactions between the adsorbent species and the adsorption solution. In addition, at higher pH, the competition between ACT and hydroxyl ions for adsorption led to a decrease in the removal efficiency (Wong et al., 2018).

3.3. Effect of the adsorbent dosage

The impact of ACGT dosage on the adsorptive elimination of ACT is depicted in Fig. 9. Adsorbent dosage plays a direct role in calculating the cost of the adsorption system as well as determining the adsorption capacity of ACT on the sorbent. The results showed that the removal efficiency of ACT increased with the increase of adsorbent dose. Adsorption increased to an optimal dosage of 0.25 g showing maximum adsorption of 97.6%. This occurs due to the increased adsorption sites on ACGT with increasing a dosage. After optimal dosage, no significant increase in the adsorptive capacity was noticed (Wong et al., 2018, Kollarahithlu and Balakrishnan 2021). The results of the study by Streit et al. (2020) for the removal of ibuprofen, ketoprofen and paracetamol by activated carbon prepared from the wastewater of the beverage industry, showed that increasing the adsorbent dose increases the efficiency of the drug removal due to the increase in the number of active sites in the adsorbents (Streit et al., 2021). The results of the study performed by Wong et al. (2018) and the study done by Saied et al (2022) showed that by increasing the adsorbent dose, the removal percentage increases up to the optimal point and then it becomes constant and sometimes decreases (Wong et al., 2018, Saied et al., 2022).

3.4. Effect of initial ACT concentration

The impact of initial ACT concentration on the adsorption process by ACGT is depicted in Fig. 10.The graph clearly shows the optimum concentration as 100 mg/L with the removal of 98.74% ACT. Because by increasing the initial concentration, the driving force for mass transfer also increases and enhancing the absorption

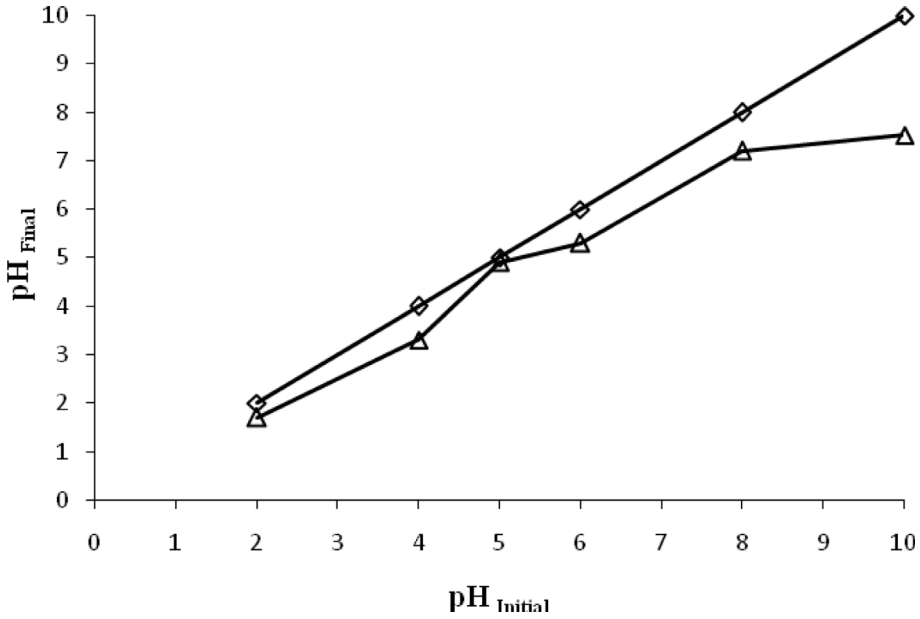

Fig. 7. Ph_{pzc} of ACGT.

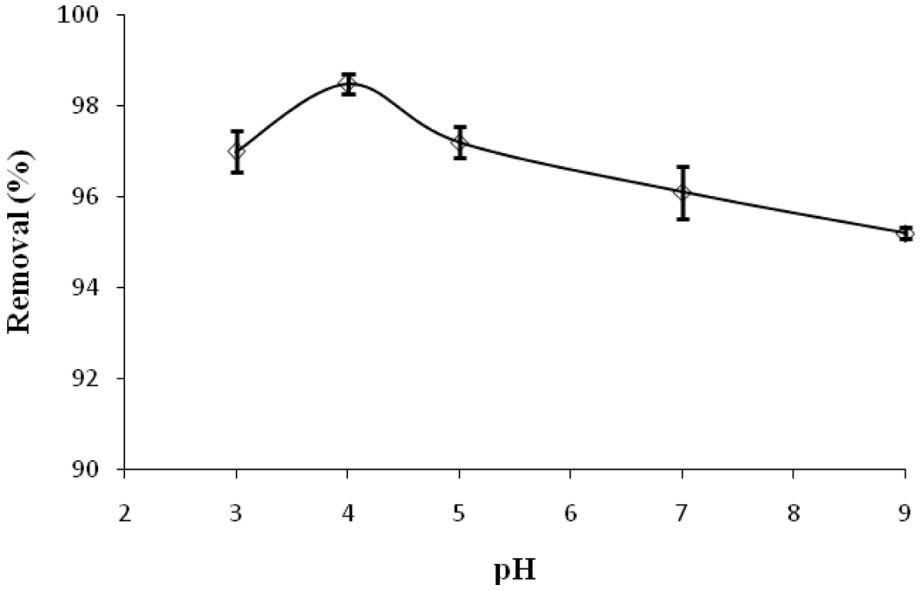

Fig. 8. Effect of pH on ACT adsorption.

rate of ACT (Dutta et al., 2015). At low concentrations, ACT molecules are attached to the active sites by attractive forces (electrostatic, van der Waals, etc.), but the mass transfer resistance between the aqueous phase and the solid phase inhibits the interaction between the adsorbent and the adsorbed solution. At higher concentrations, more molecules are capable to overcome the resistance, and as a result, more absorption takes place on the adsorbent (Wong et al., 2018). Similar results were found by Dutta et al. in 2015, showing that the removal efficiency increases with increasing ACT concentration (20–100 mg/L) and contact time (0–120 min) (Dutta et al., 2015). The results of the study by Natarajan et al. in 2022 showed that the increase in adsorption capacity (mg/g) with increasing the initial concentration of the adsorbate is possible due to the more collisions between ACT ions and adsorbent particles (Natarajan et al., 2022).

3.5. Effect of ionic strength

The effect of solution ion strength on the sorption process by ACGT is shown in Fig. 11. Ca^{2+} in the form of $CaCL_2$ was selected as the most important cation in water and the effects of concentrations 20––80 mg/L, on the level of ACT adsorption was investigated. The results of this study showed that the removal efficiency of ACT decreased with increasing the ionic strength, so the highest removal efficiency (98.45%) was observed at the concentration of 30 mg/L $CaCL_2$. This means that the high ionic strength of the solution can have competitive effects on the ACT adsorption rate. Decreasing the adsorption rate at high ionic strengths could be attributed to the increase in the concentration of competitive anions and to the decrease in the ion activity of ACT ions. Normoradi et al. (2018) reported that with increasing

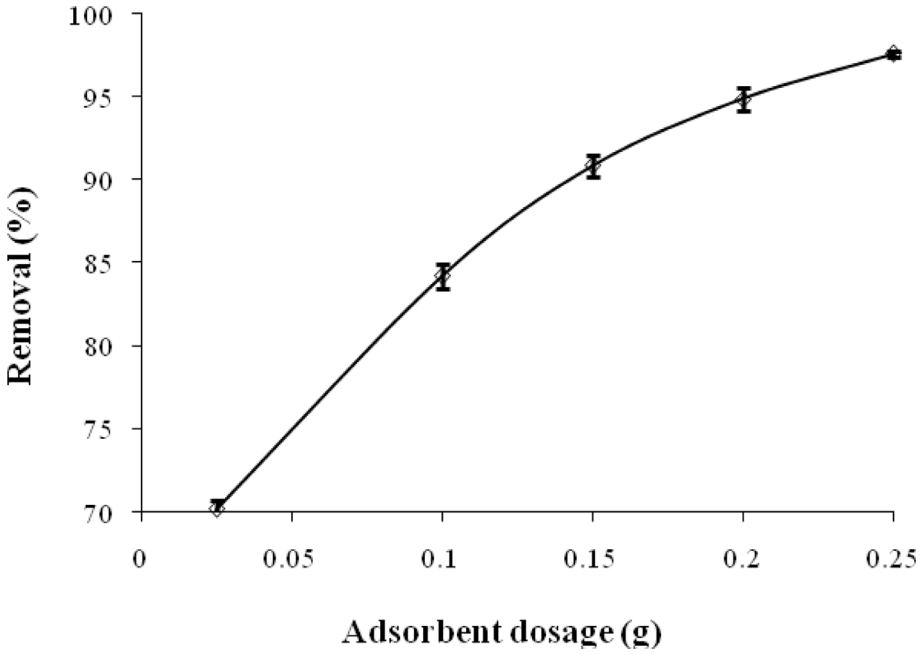

Fig. 9. Effect of adsorbent dosage on ACT adsorption.

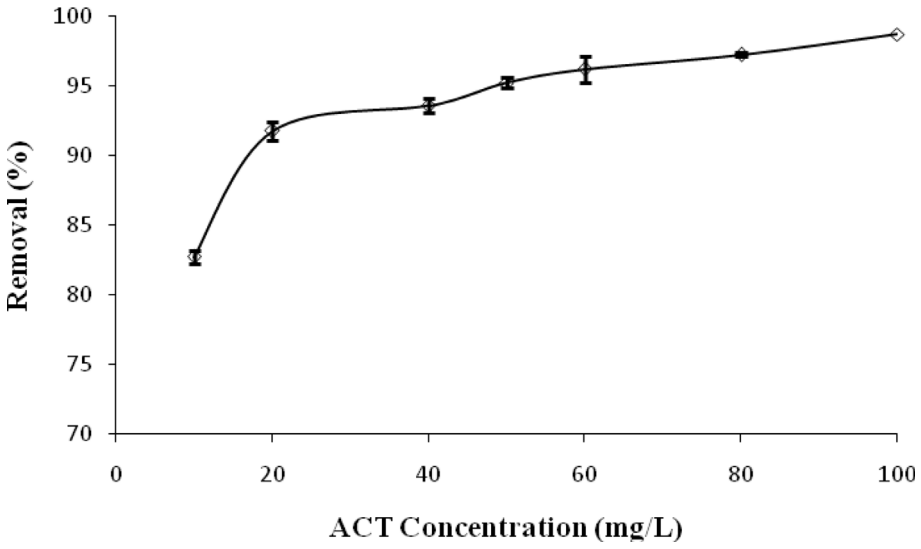

Fig. 10. Effect of initial concentration on ACT adsorption.

ion intensity, the removal efficiency of ACT and IBP decreased slightly, which may be due to the reduction of electrostatic interactions between the adsorbent and adsorbates (Nourmoradi et al., 2018). In contrast, the results of Quesada et al. (2019) study showed that the adsorption capacity of ACT was not affected by the presence of ions in the aqueous solution (Quesada et al., 2019). Because electrostatic interactions are not involved in the present study.

3.6. Effect of contact time

The experimental results of the effect of contact time on the ACT adsorption by ACGT are depicted in Fig. 12. In the present study, the highest amount of ACT removal was observed in the contact time of 30 min (98.69%). The rapid increase in adsorption capacity is due to the free active site and porous nature of the ACGT, while as time progressed gets occupied by ACT molecules (Natarajan et al., 2021). In times longer than 30 min, a positive change in ACT adsorption efficiency was not observed. This is possible due to the saturation of absorbent pores on the adsorbent surface. Hence it clearly indicates that contact time 30 min is sufficient for maximal ACT removal (Natarajan et al., 2022). The optimal contact time for ACT adsorption by silica microspheres was reported to be 30 min in the study of Natarajan et al. (2021) (Natarajan et al., 2021).

3.7. Thermodynamic studies

Gibbs free energy change (ΔG°), change in enthalpy (ΔH°) and change in entropy (ΔS°) are the thermodynamic specifications

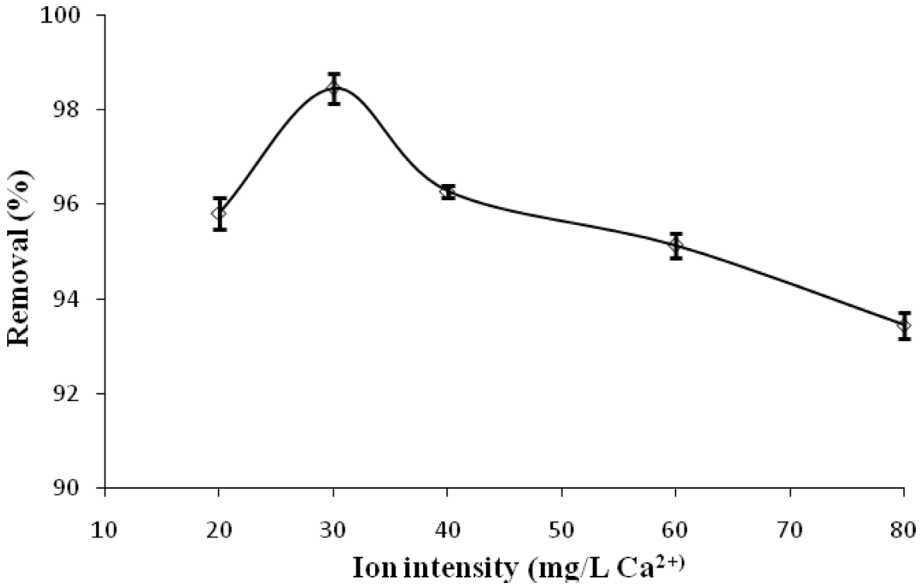

Fig. 11. Effect of ionic strength on ACT adsorption.

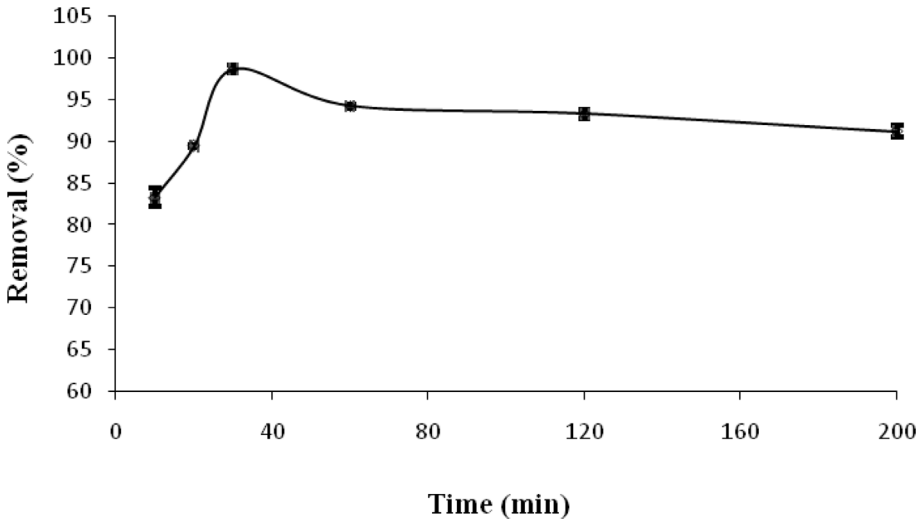

Fig. 12. Effect of contact time on ACT adsorption.

were studied for the adsorptive action of the pollutant onto ACGT. The energetic changes and the fundamental mechanism in the adsorption process are described by these three parameters (Inyinbor et al., 2023). Thermodynamic studies were performed at 288 K, 298 K, 308 K and 318 K. Thermodynamic parameters are listed in Table 2. The negative value of ΔG° in this study indicates towards the feasibility and spontaneity of adsorption of ACT onto ACGT. The values of ΔG° indicate that physical forces like Van der Waal's, hydrogen bonding and dipole–dipole interactions may be involved in the adsorption of ACT onto ACGT (Lung et al., 2021). The value of ΔH° was found to be 9.2 kJ/mol which indicated that the adsorption of ACT on ACGT was endothermically driven process. The value of ΔS° was found to be 43.58 k J/mol which suggested the randomness on the sorbent/solution interphase. The values of ΔH° obtained for ACT (9.16 kJ mol^{-1}) was positive, indicating the endothermic nature of the adsorption process. The result of Rahman et al. (2020) study consistent with the results obtained here in (Rahman and Nasir 2020).

Table 2
Thermodynamic parameters for ACT adsorption on ACGT.

Adsorbent	ΔG (kJ/mol)				ΔH/R	ΔH	ΔS/R	ΔS
	283	298	303	318				
ACGT	−3.4	−3.83	−4.3	−4.7	1102.4	9.16	5.24	43.58

3.8. Adsorption isotherms

Adsorption isotherms are used to understand how the adsorbate molecules are partitioned between the aqueous and solid phases under equilibrium condition (Conde-Cid et al., 2021). The equilibrium experimental data of ACGT adsorption were analyzed by Langmuir, Freundlich and Dubinin–Radushkevich models. The Langmuir isotherm assumes that the adsorbate molecules form a monolayer on adsorbents with homogeneous surface, while Freundlich isotherm describes a multilayer adsorption onto heteroge-

Table 3
Isotherm parameters for ACT adsorption on ACGT.

Adsorbate	Langmuir isotherm			Freundlich isotherm			D-R isotherm		
	Q_m(mg/g)	b(l/mg)	R^2	K_f (l/g)	n	R^2	q_m(mg/g)	E (kJ/mol)	R^2
ACGT	14.34	0.46	0.91	4.25	1.31	**0.97**	5.88	2.46	0.91

Table 4
Kinetic parameters forACT adsorption on ACGT.

Parameters	Pseudo-first order			Pseudo-second order			Intraparticle diffusion		
	q_e (mg/g)	K	R^2	q_e (mg/g)	K	R^2	C	K	R^2
ACGT	0.27	0.88	0.8712	7.22	1.70	**0.988**	7.97	0.369	0.363

neous surfaces (Reddy et al., 2023). According to Table 3, the ACT adsorption data were well fitted by Freundlich isotherm model (R^2 = 0.97). The n parameter of the Freundlich equation indicates the reactivity and heterogeneity of the active sites of an adsorbent. If n = 1 the adsorption is linear, if n > 1 the adsorption process is mainly chemical, and if n < 1 it indicates that physical adsorption is more favorable. In the present study, n value was 1.31 which indicates a high affinity of ACT for adsorption sites, and also a high binding energy. A similar result was reported by Natarajan et al. (2021) for ACT removal from wastewater using silica microspheres (Natarajan et al., 2021).

3.9. Adsorption kinetics

For a comprehensive understanding of adsorption dynamics, it is necessary to do a kinetic study (Mohammadi-Moghadam et al., 2013). To examine and interpret the adsorptive process, the following three models for adsorption kinetics, pseudo-first-order kinetics and pseudo-second-order kinetics were employed. Kinetic and intraparticle diffusion model parameters of ACT adsorption onto ACGT are given in Table 4. On comparing the three models, the experimental data of ACT adsorption onto ACGT were also well fitted by Pseudo-second order model and the evaluated qe value (7.2 mg/g) is near to the experimental data (7.9 mg/g). This also proved that the uptake mechanism is chemisorption. The intraparticle diffusion model is also implemented, but the adsorption plot was not linear over the whole-time range for the studied concentrations. Natarajan et al. (2022) and Rahman et al (2020) were reported similar results (Rahman and Nasir 2020, Natarajan et al., 2022).

4. Conclusion

The present research investigated a new activated carbon derived from Gundelia tournefortii seeds for effective removal of ACT from aqueous solutions. The adsorption of ACT onto ACGT was dependent on pH, adsorbent dose, contact time, initial concentration and Ca $^{2+}$ ionic strength. FESEM, EDX, XRD, FTIR, BET, TGA techniques, and pHzpc experiment were employed to characterize the newly synthesized adsorbent. The optimum conditions for ACT removal on the ACGT were: 100 mg/L initial ACT concentration, pH 4, 30 min contact time, 0.25 g/L adsorbent dose and temperature 25 °C.Adsorption kinetics and isotherms followed a pseudo second order and Freundlich models respectively. Thermodynamic studies at various temperatures indicated that the adsorption process was spontaneous and endothermic. Conclusively, this experimental study emphasized the efficiency of ACGT as an effective, eco-friendly, and economically viable adsorbent for the removal of ACT from aqueous solutions. More research on the disposal of used adsorbent is essential to ensure that it does not cause additional environmental problems.

Ethical approval

The current study was approved by the Medical Ethics Committee of Shahrekord University of Medical Sciences (IR.SKUMS. Rec.1401.028).

Declaration of Competing Interest

The authors declare that they have no known competing financial interests or personal relationships that could have appeared to influence the work reported in this paper.

Acknowledgements

We gratefully acknowledge the financial support by research deputy of Shahrekord University of Medical Sciences [Grant Number: 6044] and the collaboration of Laboratory of Health Faculty.

Appendix A. Supplementary data

Supplementary data to this article can be found online at https://doi.org/10.1016/j.arabjc.2023.105253.

References

Ahmed, E.-S.-A.-E., El-Sayed, B.A., Mohamed, W.A.A., et al., 2021. Recycling of supported nanocomposites for hazardous industrial wastewater treatment via Solar photocatalytic process. Egypt. J. Pet. 30, 29–35 10.1016/j.ejpe.2021.02.001.

Akay, C., Tezel, U., 2020. Biotransformation of Acetaminophen by intact cells and crude enzymes of bacteria: A comparative study and modelling. Sci. Total Environ. 703, 134990.

Ali, N.S., Jabbar, N.M., Alardhi, S.M., et al., 2022. Adsorption of methyl violet dye onto a prepared bio-adsorbent from date seeds: Isotherm, kinetics, and thermodynamic studies. Heliyon. 8, e10276.

Alorabi, A.Q., Hassan, M.S., Azizi, M., 2020. Fe3O4-CuO-activated carbon composite as an efficient adsorbent for bromophenol blue dye removal from aqueous solutions. Arab. J. Chem. 13, 8080–8091.

Amouzgar, P., Chan, E.-S., Salamatinia, B., 2017. Effects of ultrasound on development of Cs/NAC nano composite beads through extrusion dripping for acetaminophen removal from aqueous solution. J. Clean. Prod. 165, 537–551.

Baccar, R., Sarrà, M., Bouzid, J., et al., 2012. Removal of pharmaceutical compounds by activated carbon prepared from agricultural by-product. Chem. Eng. J. 211, 310–317.

Bello, O.S., Moshood, M.A., Ewetumo, B.A., et al., 2020. Ibuprofen removal using coconut husk activated Biomass. Chem. Data Collect. 29, 100533.

Conde-Cid, M., Cela-Dablanca, R., Ferreira-Coelho, G., et al., 2021. Sulfadiazine, sulfamethazine and sulfachloropyridazine removal using three different porous materials: Pine bark, "oak ash" and mussel shell. Environ. Res. 195, 110814.

Cunha, M.R., Lima, E.C., Lima, D.R., et al., 2020. Removal of captopril pharmaceutical from synthetic pharmaceutical-industry wastewaters: Use of activated carbon derived from Butia catarinensis. J. Environ. Chem. Eng. 8, 104506.
Dadkhah, A., Khalaj, G., Fatemi, F., et al., 2016. Evaluation the role of Ferula gummosa essential oil against the hepatoxicity induced by acetaminophen in animal model. Journal of Medicinal Plants. 15, 14–23.
Darweesh, M.A., Elgendy, M.Y., Ayad, M.I., et al., 2022. Adsorption isotherm, kinetic, and optimization studies for copper (II) removal from aqueous solutions by banana leaves and derived activated carbon. S. Afr. J. Chem. Eng. 40, 10–20.
Dutta, M., Das, U., Mondal, S., et al., 2015. Adsorption of acetaminophen by using tea waste derived activated carbon. Int. J. Environ. Sci. 6, 270–281.
Eichenbaum, G., Yang, K., Gebremichael, Y., et al., 2020. Application of the DILIsym® Quantitative Systems Toxicology drug-induced liver injury model to evaluate the carcinogenic hazard potential of acetaminophen. Regul. Toxicol. Pharm. 118, 104788.
Eslami, A., Chegini, Z.G., Khashij, M., et al., 2020. Removal of acetaminophen (ACT) from aqueous solution by using nanosilica adsorbent: experimental study, kinetic and isotherm modeling. Pigm. Resin Technol.
Fahmy, A., Mohamed, T.A., Friedrich, J.F., 2018. XPS and IR studies of plasma polymers layer deposited from allylamine with addition of ammonia. Appl. Surf. Sci. 458, 1006–1017 10.1016/j.apsusc.2018.07.160.
Fahmy, A., El-Zomrawy, A., Saeed, A.M., et al., 2020a. Degradation of organic dye using plasma discharge: optimization, pH and energy. Plasma Research Express. 2,. https://doi.org/10.1088/2516-1067/ab6703 015009.
Fahmy, A., Mohamed, T.A., Abu-Saied, M., et al., 2020b. Structure/property relationship of polyvinyl alcohol/dimethoxydimethylsilane composite membrane: Experimental and theoretical studies. Spectrochim. Acta A Mol. Biomol. Spectrosc. 228, 10.1016/j.saa.2019.117810 117810.
Fahmy, A., Anis, B., Szymoniak, P., et al., 2022. Graphene Oxide/Polyvinyl Alcohol–Formaldehyde Composite Loaded by Pb Ions: Structure and Electrochemical Performance. Journal 14. https://doi.org/10.3390/polym14112303.
González-Hourcade, M., dos Reis, G.S., Grimm, A., et al., 2022. Microalgae biomass as a sustainable precursor to produce nitrogen-doped biochar for efficient removal of emerging pollutants from aqueous media. J. Clean. Prod. 348, 131280.
Hajizadeh-Sharafabad, F., Alizadeh, M., Mohammadzadeh, M.H.S., et al., 2016. Effect of Gundelia tournefortii L. extract on lipid profile and TAC in patients with coronary artery disease: a double-blind randomized placebo controlled clinical trial. Journal of Herbal Medicine. 6, 59–66.
Inbaraj, B.S., Sridhar, K., Chen, B.-H., 2021. Removal of polycyclic aromatic hydrocarbons from water by magnetic activated carbon nanocomposite from green tea waste. J. Hazard. Mater. 415, 125701.
Inyinbor, A.A., Bankole, D.T., Adekola, F.A., et al., 2023. Chemometrics validation of adsorption process economy: Case study of acetaminophen removal onto quail eggshell adsorbents. Scientific African. 19, e01471.
Iovino, P., Canzano, S., Capasso, S., et al., 2015. A modeling analysis for the assessment of ibuprofen adsorption mechanism onto activated carbons. Chem. Eng. J. 277, 360–367.
Kekes, T., Nika, M.-C., Tsopelas, F., et al., 2020. Use of δ-manganese dioxide for the removal of acetaminophen from aquatic environment: Kinetic–thermodynamic analysis and transformation products identification. J. Environ. Chem. Eng. 8, 104565.
Khalil, H., Jawaid, M., Firoozian, P., et al., 2013. Activated carbon from various agricultural wastes by chemical activation with KOH: preparation and characterization. J. Biobaased Mater. Bioenergy 7, 708–714.
Kharrazi, S.M., Soleimani, M., Jokar, M., et al., 2021. Pretreatment of lignocellulosic waste as a precursor for synthesis of high porous activated carbon and its application for Pb (II) and Cr (VI) adsorption from aqueous solutions. Int. J. Biol. Macromol. 180, 299–310.
Klasson, K.T., Ledbetter, C.A., Wartelle, L.H., et al., 2010. Feasibility of dibromochloropropane (DBCP) and trichloroethylene (TCE) adsorption onto activated carbons made from nut shells of different almond varieties. Ind. Crop Prod. 31, 261–265.
Kollarahithlu, S.C., Balakrishnan, R.M., 2021. Adsorption of pharmaceuticals pollutants, Ibuprofen, Acetaminophen, and Streptomycin from the aqueous phase using amine functionalized superparamagnetic silica nanocomposite. J. Clean. Prod. 294, 126155.
Kumari, S., Kumar, R.N., 2021. River water treatment using electrocoagulation for removal of acetaminophen and natural organic matter. Chemosphere 273, 128571.
Liu, W.-J., Zeng, F.-X., Jiang, H., et al., 2011. Preparation of high adsorption capacity bio-chars from waste biomass. Bioresour. Technol. 102, 8247–8252.
Lung, I., Soran, M.-L., Stegarescu, A., et al., 2021. Evaluation of CNT-COOH/MnO2/Fe3O4 nanocomposite for ibuprofen and paracetamol removal from aqueous solutions. J. Hazard. Mater. 403, 123528.
Marcelino, G.R., de Carvalho, K.Q., de Lima, M.X., et al., 2020. Construction waste as substrate in vertical subsuperficial constructed wetlands treating organic matter, ibuprofenhene, acetaminophen and ethinylestradiol from low-strength synthetic wastewater. Sci. Total Environ. 728, 138771.
Mestre, A.S., Pires, J., Nogueira, J.M., et al., 2009. Waste-derived activated carbons for removal of ibuprofen from solution: role of surface chemistry and pore structure. Bioresour. Technol. 100, 1720–1726.
Mohamed, W.A.A., Fahmy, A., Helal, A., et al., 2022. Degradation of local Brilliant Blue R dye in presence of polyvinylidene fluoride/MWCNTs/TiO2 as photocatalysts and plasma discharge. J. Environ. Chem. Eng. 10, 10.1016/j.jece.2021.106854 106854.
Mohammadi-Moghadam, F., Amin, M. M., Momenbeik, F. et al., 2013. Application of Glycyrrhiza glabra root as a novel adsorbent in the removal of toluene vapors: Equilibrium, kinetic, and thermodynamic study. Journal of environmental and public health. 2013.
Mohan, D., Sarswat, A., Singh, V.K., et al., 2011. Development of magnetic activated carbon from almond shells for trinitrophenol removal from water. Chem. Eng. J. 172, 1111–1125.
Mojiri, A., Vakili, M., Farraji, H., et al., 2019. Combined ozone oxidation process and adsorption methods for the removal of acetaminophen and amoxicillin from aqueous solution; kinetic and optimisation. Environ. Technol. Innov. 15, 100404.
Natarajan, R., Banerjee, K., Kumar, P.S., et al., 2021. Performance study on adsorptive removal of acetaminophen from wastewater using silica microspheres: Kinetic and isotherm studies. Chemosphere 272, 129896.
Natarajan, R., Kumar, M.A., Vaidyanathan, V.K., 2022. Synthesis and characterization of rhamnolipid based chitosan magnetic nanosorbents for the removal of acetaminophen from aqueous solution. Chemosphere 288, 132532.
Norouzi, S., Heidari, M., Alipour, V., et al., 2018. Preparation, characterization and Cr (VI) adsorption evaluation of NaOH-activated carbon produced from Date Press Cake; an agro-industrial waste. Bioresour. Technol. 258, 48–56.
Nourmoradi, H., Moghadam, K.F., Jafari, A., et al., 2018. Removal of acetaminophen and ibuprofen from aqueous solutions by activated carbon derived from Quercus Brantii (Oak) acorn as a low-cost biosorbent. J. Environ. Chem. Eng. 6, 6807–6815.
Ouyang, J., Zhou, L., Liu, Z., et al., 2020. Biomass-derived activated carbons for the removal of pharmaceutical mircopollutants from wastewater: A review. Sep. Purif. Technol. 253, 117536.
Parus, A., Gaj, M., Karbowska, B., et al., 2020. Investigation of acetaminophen adsorption with a biosorbent as a purification method of aqueous solution. Chem. Ecol. 36, 705–725.
Quesada, H.B., Cusioli, L.F., Bezerra, C. de O, et al., 2019. Acetaminophen adsorption using a low-cost adsorbent prepared from modified residues of Moringa oleifera Lam. seed husks. J. Chem. Technol. Biotechnol. 94, 3147–3157.
Rahman, N., Nasir, M., 2020. Effective removal of acetaminophen from aqueous solution using Ca (II)-doped chitosan/β-cyclodextrin composite. J. Mol. Liq. 301, 112454.
Reddy, Y.S., Rotte, N.K., Hussain, S., et al., 2023. Sustainable mesoporous graphitic activated carbon as biosorbent for efficient adsorption of acidic and basic dyes from wastewater: Equilibrium, kinetics and thermodynamic studies. Journal of Hazardous Materials Advances. 9, 100214.
Saied, M.E., Shaban, S.A., Mostafa, M.S., et al., 2022. Efficient adsorption of acetaminophen from the aqueous phase using low-cost and renewable adsorbent derived from orange peels. Biomass Convers. Biorefin., 1–18
Silva, T.L., Cazetta, A.L., Souza, P.S., et al., 2018. Mesoporous activated carbon fibers synthesized from denim fabric waste: efficient adsorbents for removal of textile dye from aqueous solutions. J. Clean. Prod. 171, 482–490.
Streit, A.F., Collazzo, G.C., Druzian, S.P., et al., 2021. Adsorption of ibuprofen, ketoprofen, and paracetamol onto activated carbon prepared from effluent treatment plant sludge of the beverage industry. Chemosphere 262, 128322.
Thabede, P.M., Shooto, N.D., Naidoo, E.B., 2020. Removal of methylene blue dye and lead ions from aqueous solution using activated carbon from black cumin seeds. S. Afr. J. Chem. Eng. 33, 39–50.
Wong, S., Lim, Y., Ngadi, N., et al., 2018. Removal of acetaminophen by activated carbon synthesized from spent tea leaves: equilibrium, kinetics and thermodynamics studies. Powder Technol. 338, 878–886.
Xue, H., Wang, X., Xu, Q., et al., 2022. Adsorption of methylene blue from aqueous solution on activated carbons and composite prepared from an agricultural waste biomass: A comparative study by experimental and advanced modeling analysis. Chem. Eng. J. 430, 132801.
Yang, Q., Huang, H., Li, K., et al., 2021. Ibuprofen removal from drinking water by electro-peroxone in carbon cloth filter. Chem. Eng. J. 415, 127618.
Yosef, M., Fahmy, A., Hotaby, W.E., et al., 2020. High performance graphene-based PVF foam for lead removal from water. J. Mater. Res. Technol. 9, 11861–11875 10.1016/j.jmrt.2020.08.011.
Yosef, M., Fahmy, A., Hassan, A., et al., 2021. Porous Polyvinyl Formaldehyde / MWCNTs Foam for Pb+2 Removal from Water. Egypt. J. Chem. 64, 533–545 10.21608/ejchem.2020.34453.2733.
Żółtowska-Aksamitowska, S., Bartczak, P., Zembrzuska, J., et al., 2018. Removal of hazardous non-steroidal anti-inflammatory drugs from aqueous solutions by biosorbent based on chitin and lignin. Sci. Total Environ. 612, 1223–1233.